Research on the Constitutive Mathematical Model of Ti60 Titanium Alloy and Isothermal Forging Forming Simulation

Xiaohua Wang, Lintao Chen, Guangyong Pan, Yongjie Qi

School of Intelligent Manufacturing, Zhejiang Guangsha Vocational and Technical University of Construction, Dongyang, 322100, China

Abstract

To optimize the isothermal β forging process of Ti60 titanium alloy ring disk parts, this study focuses on the alloy ring-disk as the research subject. Using JMatPro software, the flow stress curves and thermophysical parameters under temperatures of 1000-1200°C and strain rates of 0.001-0.1 s-1 were calculated, and a flow stress constitutive mathematical model was fitted. Based on DEFORM-3D finite element software, the forging die and blank of the ring-disk were designed, and the isothermal forging process under deformation temperatures of 1060-1120℃ and strain rates of 0.001-0.01 s-1 was simulated. The effects of deformation conditions on effective strain, equivalent stress, and forming load were analyzed. The results indicate that the flow stress of Ti60 titanium alloy decreases with increasing deformation temperature and decreasing strain rate. During deformation, strain initially concentrates in the die contact area and later expands toward the center, with the load rapidly increasing in the final stage of forming. Lower strain rates (0.001 s-1) and higher deformation temperatures (1120℃) reduce material deformation resistance, promote more uniform stress distribution, and improve the forming quality of the forging. This study provides numerical simulation references for the thermal working process formulation of Ti60 titanium alloy ring disk parts.

Keywords

Ti60 Titanium Alloy; Isothermal Forging; Constitutive Mathematical Model; Finite Element Simulation; Ring Disk Components; Flow Stress.

1. Introduction

Ti60 titanium alloy is a nearly α type high-temperature titanium alloy with excellent comprehensive performance. Compared with other high-temperature titanium alloys such as TC11 and TC17 in China, it has better creep resistance when working in environments above 500°C, and is suitable for the manufacturing of aviation high-pressure gas turbine blades, casings and other components [1-2].

Isothermal forging is its main processing method. Isothermal forging is the process of heating a mold and billet together to a deformation temperature and deforming them at a lower strain rate to achieve precision forming of the forging. For large, complex, and difficult to deform materials, isothermal forging has great advantages. Scholars have conducted research on the isothermal deformation process of Ti60 titanium alloy. Wang Tao et al. [4] studied the effect of isothermal forging strain rate on the microstructure and properties of Ti60 alloy based on thermal compression tests; Mao Zhiyong et al. [5] studied the effect of isothermal forging temperature on the microstructure and room temperature tensile properties of Ti60 alloy based on thermal compression tests; Wang et al. [3] studied the rheological behavior and plastic deformation mechanism of Ti60 alloy based on thermal compression tests. It is known that research on deformation technology is mostly based on cylindrical thermal compression tests, but with the development of computer technology and numerical calculation methods, finite element numerical simulation has become an effective method for analyzing plastic forming problems [6]. The combination of experiments and simulations can simulate the actual forging process under different deformation conditions, observe the deformation laws of various parts of the forging, and effectively save time and costs.

JMatPro, as a metal material performance calculation software, establishes different theoretical models based on thermodynamic calculations and performance databases to calculate various material properties [7], including solidification and thermal properties such as thermal conductivity, Young's modulus, surface tension, etc; Mechanical properties include strength and hardness, stress-strain curve, forming limit diagram, fracture toughness, etc; The phase transition kinetics include TTT curve, CCT curve, precipitation and isothermal aging.

This article takes the isothermal β forging process of Ti60 titanium alloy ring disk parts as the research object, combined with JMatPro material performance simulation software and commercial DEFORM-3D finite element software [8], to study the influence of different deformation conditions on die forgings. In order to provide guidance for the development of thermal working processes for related ring and disk components.

2. Experimental Materials and Methods

The experimental material is Ti60 titanium alloy rod provided by a certain aviation forging and casting plant. The material composition is shown in Table 1. The room temperature equilibrium microstructure is mainly composed of alpha phase and a small amount of beta phase, and the transition point from alpha to beta phase is 1050 ℃± 5 ℃. As a nearly alpha type high-temperature titanium alloy, Ti60 titanium alloy's alloying design is in line with the research and development trend of high-temperature titanium alloys [9], and it has excellent high-temperature mechanical properties.

Table 1. Composition of Ti60 Titanium Alloy Material (%)

Al	Sn	Zr	Mo	Ta	Si	Nb	C
5.6	3.7	3.2	0.5	1.0	0.37	0.4	0.05

Use JMatPro material performance simulation software to calculate the thermodynamic parameters of Ti60 titanium alloy. Firstly, input the chemical composition of the material into the software, and calculate the flow stress curve and thermal properties parameters based on its model and performance database [7]. The deformation conditions are temperature T=1000-1200 ℃, strain rate=0.001-0.1s^{-1}, and strain variable=1. The flow stress equation is obtained by linear fitting the curve. The thermal properties parameters are shown in Table 2. Input the calculated flow stress equation and thermal properties parameters into the DEFORM-3D finite element software for isothermal β forging simulation of Ti60 titanium alloy ring disk components [8]. The deformation temperatures T are selected as 1060, 1090, and 1120 ℃, and the strain rates are selected as 0.001, 0.005, and 0.01s^{-1}.

Table 2. Thermal Properties of Ti60 Titanium Alloy

Young's modulus/MP	Poisson's ratio	Thermal expansion/K^{-1}	Thermal Conductivity/W/(m.K)	Heat capacity/N/mm^2/K	Emissivity
61790.10	0.382	1.235×10^{-5}	22.92	2.856	0.7

3. Ti60 Titanium Alloy Flow Stress Curve

The flow stress curve calculated based on JMatPro material performance simulation software is shown in Fig. 1. It can be inferred that at the same deformation temperature, the flow stress decreases

Volume 12 Issue 3, 2026
DOI: 10.6919/ICJE.202603_12(3).0020

with the decrease of strain rate; At the same strain rate, the flow stress decreases with the increase of deformation temperature, and reaches its maximum at small strains before slowly decreasing. This is due to the initial compression of the sample, which undergoes strain hardening and a rapid increase in stress, causing the dislocation density of the internal structure of the material to reach a critical value. Subsequently, dynamic recrystallization or dynamic recovery occurs, resulting in a decrease or slowing down of the flow stress. This change pattern is consistent with the high-temperature rheological properties of near alpha titanium alloys [10].

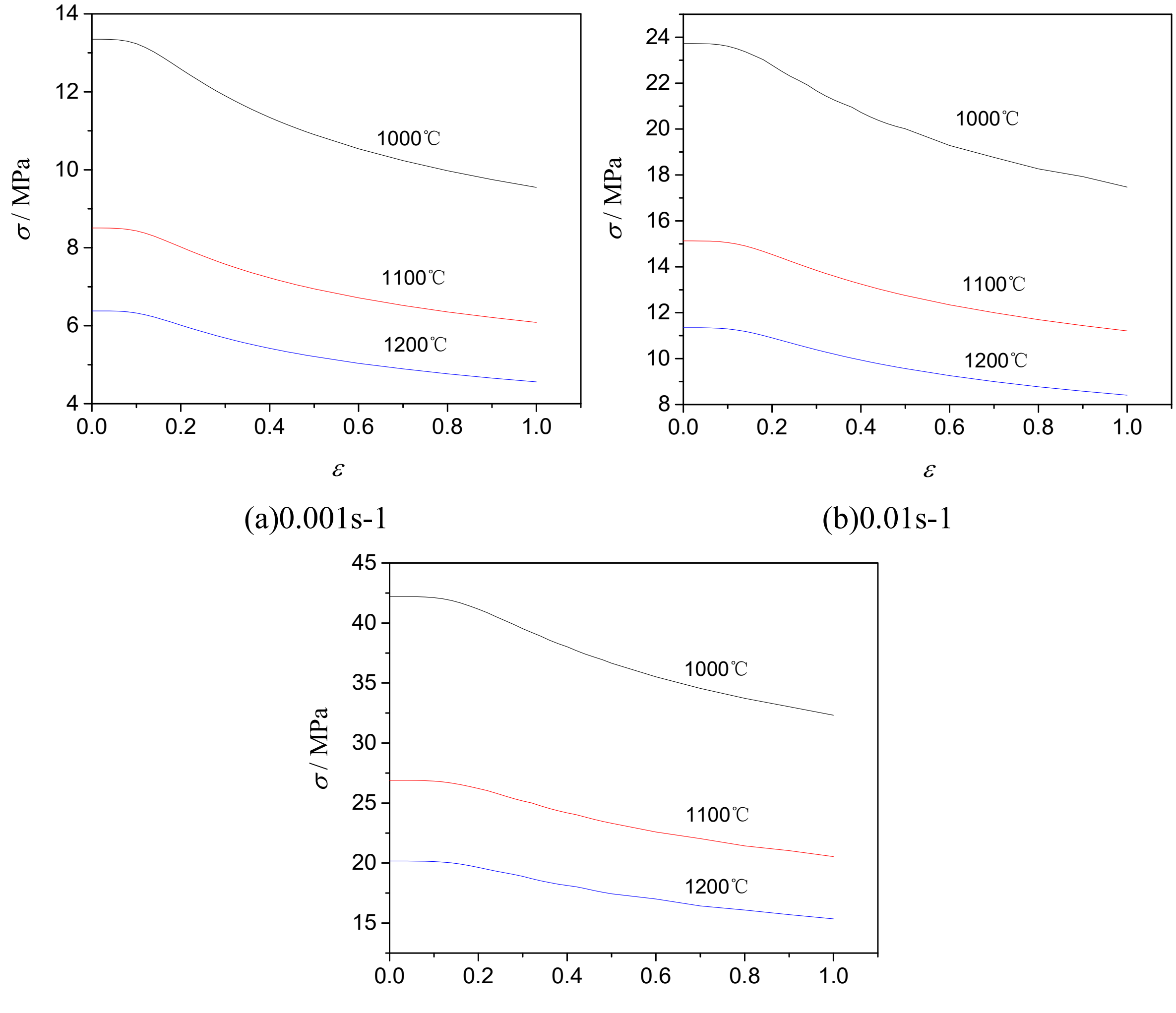

Fig.1 True stress-strain curves of Ti60 titanium alloy at different strain rates and deformation temperatures

4. Ti60 Titanium Alloy Constitutive Mathematical Model

Ti60 titanium alloy heat deformation process of flow stress with the temperature, strain rate and other rules of change can be used Arrhenius flow stress mathematical equation to indicate that[3]:

$$\dot{\varepsilon}=A[\sinh(\alpha\sigma)]^{n}\exp\left(-Q/RT\right) \tag{1}$$

Where: is the strain rate, s^{-1}; σ is the high-temperature flow stress, MPa; T is the thermal deformation temperature, K; Q is the deformation activation energy, $J.mol^{-1}$; R is the gas constant, R = 8.314 J/(mol.k); α is the stress level constant; A and n are constants.

ISSN: 2414-1895 DOI: 10.6919/ICJE.202603_12(3).0020

For different stress states, the relationship between flow stress and strain rate can be expressed by the following equation:

$$\dot{\varepsilon} = A_1\sigma^{n_1} \text{ (low level stress)} \tag{2}$$

$$\dot{\varepsilon} = A_2 \exp(\beta\sigma) \text{ (High level of stress)} \tag{3}$$

Where:A_1, A_2, β, n_1 are material constants. Where the relationship between the stress level constant a and β, n_1 can be expressed by the following equation:

$$\alpha = \frac{\beta}{n_1} \tag{4}$$

Solving for each of the constants in Eq. (1), the value of α can be found first, so taking the natural logarithm of Eq. (2) and Eq. (3) yields the following equation:

$$\ln\dot{\varepsilon} = n_1 \ln\sigma + \ln A_1 \tag{5}$$

$$\ln\dot{\varepsilon} = \beta\sigma + \ln A_2 \tag{6}$$

From Eq. (5) and Eq. (6), the value of constant n_1 is the slope of the lnσ- $\ln\dot{\varepsilon}$ relationship curve, and the value of β is the slope of the σ- $\ln\dot{\varepsilon}$ relationship curve. Therefore, we can statistically calculate the peak stress σ_p under different heat deformation conditions of cast 6061 aluminum alloy, fit and draw the relationship curves between the peak stress σ_p and the strain rate $\dot{\varepsilon}$.

Taking the natural logarithm on both sides of equation (1) yields:

$$\ln\dot{\varepsilon} = n\ln[\sinh(\alpha\sigma)] + \ln A - Q / RT \tag{7}$$

When the temperature must be a constant, a partial derivation of equation (7) yields:

$$n = [\frac{\partial \ln\dot{\varepsilon}}{\partial \ln[\sinh(\alpha\sigma)]}]_T \tag{8}$$

Calculating the fitted $\ln\dot{\varepsilon}$ and $\ln[\sinh(\alpha\sigma_p)]$ data , taking the average of the slopes gives n.

When the strain rate must be constant, a partial derivation of Eq. (7)1/T yields:

$$\frac{Q}{Rn} = [\frac{\partial \ln[\sinh(\alpha\sigma)]}{\partial(1/T)}]_{\dot{\varepsilon}} \tag{9}$$

Calculate the fit $\ln[\sinh(\alpha\sigma_p)]$ and 1/T data, take the average value of the slope can be obtained $Q/(Rn)$, the n value can be substituted into the cast 6061 aluminum alloy heat distortion activation energy Q, at the same time, it can be known that the $\ln\dot{\varepsilon}$ and $\ln[\sinh(\alpha\sigma_p)]$ the relationship between the curve intercept for the value of $\ln A\text{-}Q/RT$, for the calculation of the average value can be obtained A.

Eq. (1) by substituting the obtained values of Q, n, A and a, we can obtain the flow stress mathematical equations of Ti60 titanium alloy during heat deformation at different strain rates from 1000℃ to 1200℃.

$$\dot{\varepsilon} = 3.4859\times10^{24}\left[\sinh(0.0102\sigma)\right]^{3.8599}\exp\left[-6.8405\times10^{5}/(RT)\right] \tag{10}$$

5. Ti60 Titanium Alloy Ring Disk Forging and Mold Design

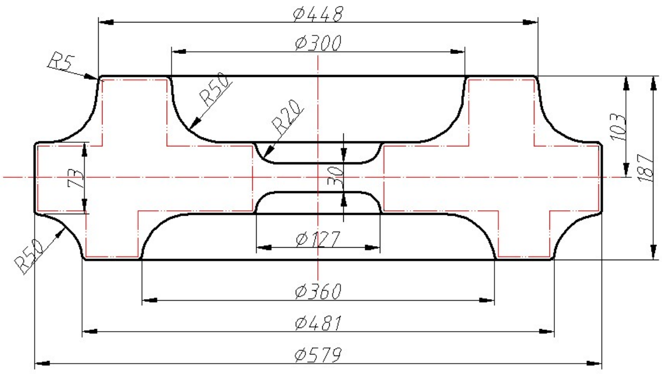

Fig. 2 Ti60 titanium alloy ring disk cold forging

The cold forging diagram of Ti60 titanium alloy ring disk is shown in Fig. 2. Based on the characteristics of forging material, size, shape, etc., the forging die design manual [11] is consulted to determine the forming parting surface, draft angle, fillet radius, machining allowance and other process parameters of the forging. The plastic forming process design of Ti60 titanium alloy needs to fully consider its high-temperature deformation characteristics [12], ensuring that the mold parameters match the material deformation law.

The parting surface is generally selected at the position of the maximum projection surface of the forging, and in order to facilitate the easy removal of the forging from the mold, a flat surface is chosen as the parting surface as much as possible. In this paper, closed die forging is adopted, and the parts are formed in a closed mold cavity. Therefore, the parting surface is selected on the end face of the forging in contact with the punch, and an ejection device is designed in the lower mold. In terms of dimensional accuracy and quality indication, closed die forging can approach the product to the maximum extent compared to other forging methods, eliminating burrs. However, it cannot completely replace the original product for direct use. Therefore, the forging needs to have a certain margin for subsequent machining and forming. Based on the size of the forging, a single-sided machining margin of 3mm is selected for the forging. In order to make the forging easy to remove from the mold cavity, the internal and external draft angles need to be designed. When the depth of the mold cavity is different, it is designed according to the deep mold cavity, and finally the draft angle is selected as 7o.

Round cake forgings generally use rough forging blanks, and for complex shapes, it is advisable to use formed rough forging blanks. The purpose of billet making is to avoid folding during final forging, and to remove oxide skin, thereby improving the surface quality of the forging and extending the service life of the forging die. Therefore, when determining the size of the intermediate billet in the ring disk forging, the appropriate diameter d and height h should be selected, otherwise it will affect the forming effect of the forging, and may also result in insufficient filling and circular wrinkles. Therefore, for disc-shaped forgings, the diameter of the intermediate billet should satisfy d=(d1+d2)/2,

ISSN: 2414-1895 DOI: 10.6919/ICJE.202603_12(3).0020

that is, d1<d<d2. Based on this, the shape and size of the Ti60 titanium alloy ring disk billet are determined, as shown in Fig. 3. This billet making principle also applies to the isothermal forging process of titanium alloy rings [13].

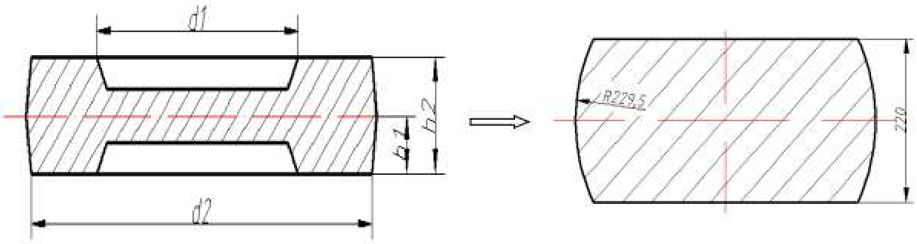

Fig. 3 Ti60 titanium alloy ring disk parts

As shown in Fig 4, the schematic diagram of the mold structure consists of an upper mold, a lower mold, and a top rod. When designing the mold cavity, it is necessary to first design the thermal forging drawing. The thermal forging drawing is based on the cold forging drawing and has some differences, that is, all dimensions on the thermal forging drawing should be included in the shrinkage rate. Compared with materials such as steel, the shrinkage rate of titanium alloy is relatively small, between 0.5% and 0.9% [12]. Use UG software to draw geometric models of molds and billets, and finally import the geometric models into DEFORM-3D software for positioning. Enter the flow stress constitutive model and thermal properties parameters in the software database, and finally simulate the isothermal forging process [8].

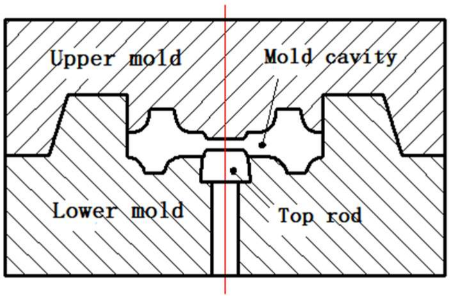

Fig.4 Schematic diagram of mold structure

6. Simulated Conditions

In the isothermal forging process, the temperature of the mold and billet should be maintained at a constant temperature, and there should be approximately no heat transfer between the mold and billet. When setting the simulation parameters, the mold can be set as a rigid component without dividing the grid, and glass lubricant with a friction factor of 0.03 is used for mold lubrication. Other simulated deformation conditions are shown in Table 3, and the effects of deformation temperature, strain rate, etc. on the forming of Ti60 titanium alloy forgings are discussed separately. The simulation parameter settings comply with the finite element simulation specification for isothermal forging of difficult to deform alloys [6].

Table 3. Simulation deformation conditions of Ti60 titanium alloy isothermal forging

No.	Temperature/℃	strain rate (s^{-1})	Percentage of deformation (%)
1	1060, 1090, 1120	0.001	100%
2	1060	0.001、0.005、0.01	

ISSN: 2414-1895 DOI: 10.6919/ICJE.202603_12(3).0020

7. Simulation Analysis of Isothermal Forging

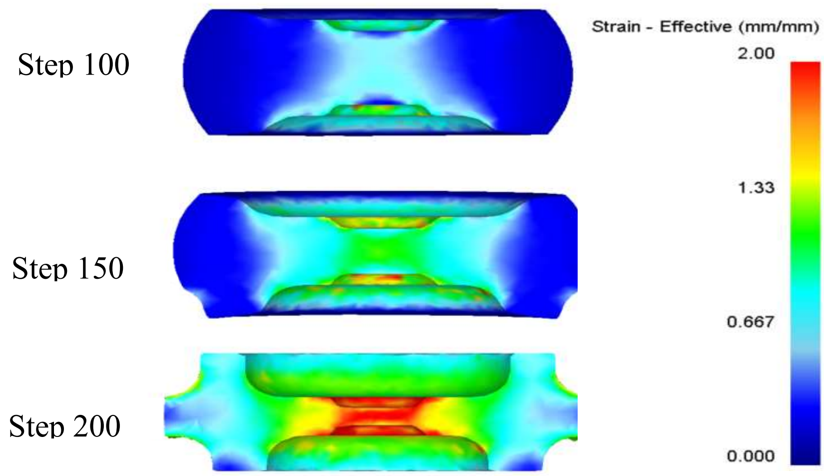

Fig.5 Effective strain distribution diagram during the forming process

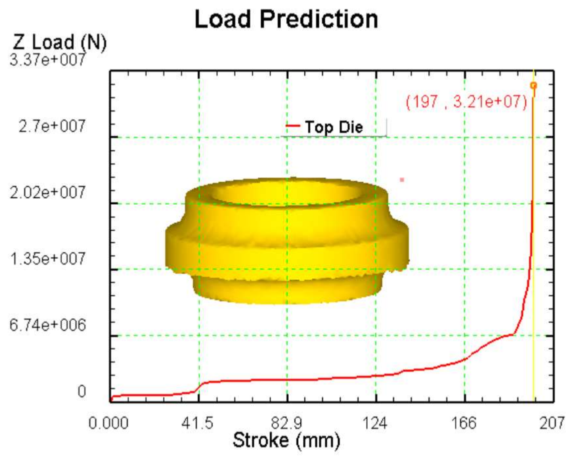

Fig.6 Stroke load curve of top die

From Fig. 5, it can be seen that there are significant changes in the distribution of effective strain corresponding to different loading steps during the forging process of Ti60 titanium alloy ring disk. In the Step 100 stage, the overall deformation of the material is relatively small, and the effective strain is mainly concentrated in the contact area between the upper and lower molds, while the middle area of the ring is still dominated by lower strain, indicating that the material mainly undergoes initial compression deformation at this time. As the forming process advances to Step 150, the strain in the contact area gradually expands towards the middle of the ring, and significant plastic flow begins to occur in the middle area. The strain distribution tends to be continuous, indicating that a stable metal flow path is gradually forming inside the material. At Step 200, there was a significant concentration of high strain in the middle region of the ring, and the maximum effective strain increased significantly, indicating that the region had undergone strong plastic deformation. At the same time, the strain distribution in the edge region was relatively low due to the outward flow of material, and the overall trend showed a gradual decrease from the center outward. Based on the convex mold stroke load curve in Fig. 6, it can be observed that as the stroke increases, the overall load shows an upward trend. In the initial stage of forming, the load growth is relatively slow due to the fact that the material is still in the initial plastic stage; As the later stage of the journey approaches the end point, the load rapidly increases and reaches about 3.21×10^{7} N, indicating a significant increase in the

ISSN: 2414-1895 DOI: 10.6919/ICJE.202603_12(3).0020

contact area between the mold and the billet. At the same time, the deformation resistance of the material increases, leading to a sharp increase in the forming load. Overall, the deformation distribution during the forging process is relatively reasonable, which can ensure the effective formation of the ring disk structure and is consistent with the deformation law of isothermal forging of titanium alloy rings [13].

Fig. 7 shows the equivalent stress distribution of Ti60 titanium alloy ring disk forgings under different deformation temperatures and strain rates. From the results of different strain rates on the left side, it can be seen that when the strain rate increases from 0.001 s^{-1} to 0.01 s^{-1}, the overall equivalent stress level of the forging significantly increases, and the high stress areas are mainly concentrated in the contact area between the upper and lower molds and the billet, as well as the deformation zone in the middle of the ring. This is mainly due to the increase in strain rate, the deformation resistance of the material increases, and the degree of plastic deformation per unit time increases, resulting in more pronounced stress concentration in local areas. Meanwhile, at higher strain rates, the internal stress distribution of the material exhibits more pronounced gradient changes, indicating that metal flow is subject to certain limitations.

From the simulation results of different deformation temperatures on the right side, it can be seen that as the temperature increases from 1060 °C to 1120 °C, the overall equivalent stress level gradually decreases, the high stress area significantly decreases, and the distribution becomes more uniform. This is because the increase in temperature will reduce the flow stress of Ti60 titanium alloy, enhance the plastic deformation ability of the material, make the metal flow smoother, and effectively alleviate the phenomenon of local stress concentration. This characteristic is related to the high-temperature creep performance of Ti60 titanium alloy [14]. Overall, lower strain rates and higher deformation temperatures are more conducive to reducing deformation resistance during forging, improving stress distribution, and helping to obtain ring disk forgings with uniform structure and fewer defects [6].

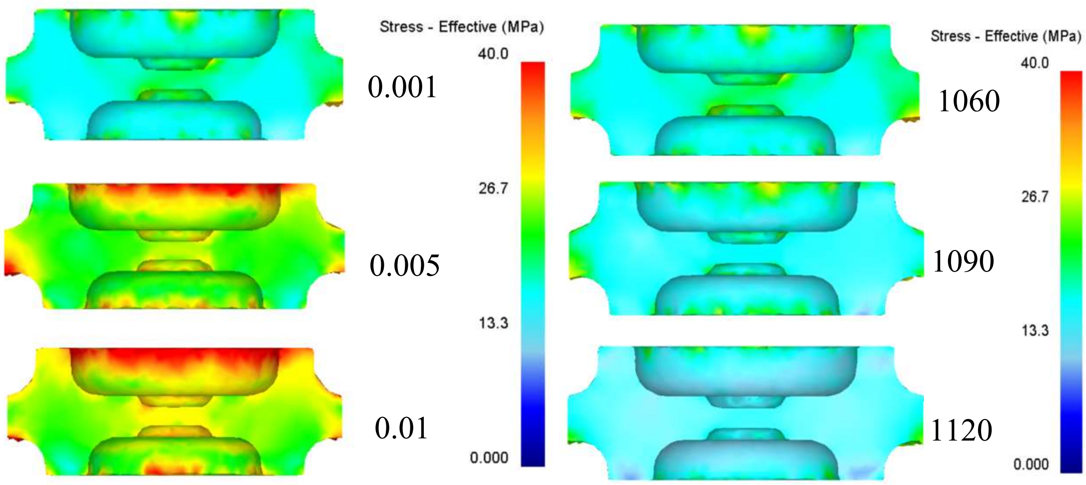

Fig.7 Effective stress distribution diagram at different deformation temperatures and strain rates

8. Conclusion

(1) The high-temperature flow stress of Ti60 titanium alloy follows the Arrhenius mathematical model law. Within the deformation temperature range of 1000-1200 °C and the strain rate range of 0.001-0.01s^{-1}, the flow stress decreases with the increase of deformation temperature, and significantly increases with the increase of strain rate. In the early stage of deformation, the strain hardening stress rapidly increases, and the stress tends to flatten after dynamic recrystallization/recovery.

(2) During the isothermal forging process of Ti60 titanium alloy ring disk parts, the effective strain gradually expands from the contact area of the mold to the middle of the ring during the forming

process. At the end of the forming process, high strain concentration occurs in the middle, and the overall strain distribution conforms to the plastic forming law. The convex mold load continues to increase with the increase of stroke, and sharply increases in the final stage.

(3) The deformation conditions have a significant impact on the forming stress of Ti60 titanium alloy ring disk parts: when the strain rate increases from 0.001s $^{-1}$ to 0.01s $^{-1}$, the overall equivalent stress of the forging increases, and local stress concentration intensifies; When the deformation temperature increases from 1060 ℃ to 1120 ℃, the flow stress of the material decreases, the plastic deformation ability increases, and the high stress area decreases and becomes more evenly distributed.

(4) By combining JMatPro material performance calculation with DEFORM-3D finite element simulation, the deformation law of Ti60 titanium alloy isothermal forging can be efficiently analyzed, greatly saving time and cost in process testing, and providing an effective method for optimizing the thermal working process of similar difficult to deform alloy complex components.

Acknowledgement

This study is the research result of visiting scholars in universities from 2025 to 2026. The author sincerely thanks Zhejiang Normal University for providing an academic research platform.

References

[1] Huang X, Li M Q, Liu J R. Research progress and application of high temperature titanium alloys[J]. Materials Review, 2018, 32(07):1164-1171.

[2] Cao C X. Application and development of titanium alloys in aerospace field[J]. Aeronautical Manufacturing Technology, 2020, 63(19):16-23.

[3] Wang K L, Xia J C, Hu G A. Flow behavior and plastic deformation mechanism of Ti60 high temperature titanium alloy during isothermal deformation[J]. Rare Metal Materials and Engineering, 2012, 41(S2):568-572.

[4] Wang T, Qu H L, Zhou Y G. Effect of strain rate on microstructure and properties of Ti60 titanium alloy during isothermal forging[J]. Hot Working Technology, 2009, 38(19):46-48.

[5] Mao Z Y, Li J M, Bai C G. Effect of isothermal forging temperature on microstructure and room temperature tensile properties of Ti60 titanium alloy[J]. Journal of Iron and Steel Research, 2011, 23(S1):401-404.

[6] Li P, Yang H, Zhan M. Finite element simulation and process optimization of isothermal forging for hard-to-deform alloys[J]. Journal of Mechanical Engineering, 2015, 51(10):71-78.

[7] Wang M, Guo H Z, Wang B Y. Application of JMatPro in simulating thermal working properties of metallic materials[J]. Hot Working Technology, 2017, 46(11):25-28.

[8] Chen M S, Liu Q K. Application skills of DEFORM-3D in forging process simulation[J]. Die & Mould Industry, 2008, 34(06):18-22.

[9] Zhang M C, Dong J X, Xie X S. Alloy design and development trend of high temperature titanium alloys[J]. Acta Metallurgica Sinica, 2019, 55(08):957-974.

[10] Yang C, Li M Q, Yu Y. Establishment and verification of high temperature flow constitutive model for near-α titanium alloy[J]. Acta Aeronautica et Astronautica Sinica, 2017, 38(02):243-252.

[11] He D X. Forging Die Design Handbook[M]. Beijing: China Machine Press, 2010.

[12] Liu J A, Sheng G M. Plastic Forming Technology and Application of Titanium Alloys[M]. Beijing: Metallurgical Industry Press, 2013.

[13] Zhou W L, Wu J J, Li F G. Numerical simulation and process optimization of isothermal forging for titanium alloy ring[J]. Journal of Plasticity Engineering, 2014, 21(03):1-6.

[14] Xu H J, Jiang Y T, Wang F. Research progress on creep properties of high temperature titanium alloys[J]. Chinese Journal of Rare Metals, 2021, 45(05):598-606.